Cell Death & Differentiation (2020) 27:1316–1327
https://doi.org/10.1038/s41418-019-0417-3

Cell Death & Differentiation

ARTICLE

LINC00265 promotes colorectal tumorigenesis via ZMIZ2 and USP7-mediated stabilization of β-catenin

Yahui Zhu[1,2] · Li Gu[1,2] · Xi Lin[1,2] · Kaisa Cui[1,2] · Cheng Liu[1,2] · Bingjun Lu[1,2] · Feng Zhou[3,4] · Qiu Zhao[3,4] · Hongxing Shen[1,2] · Youjun Li[1,2]

Received: 9 December 2018 / Revised: 19 August 2019 / Accepted: 2 September 2019 / Published online: 17 September 2019

Abstract

Colorectal cancer (CRC) is the third most prevalent world cancer and oncogenic β-catenin is frequently dysregulated in CRC. Long noncoding RNAs (lncRNAs) play critical roles in colorectal tumorigenesis; however, the contributions of lncRNAs to human CRC remain largely unknown. In this study, we report that LINC00265 is upregulated and predicts poor clinical outcome in human patients with CRC. Depletion of LINC00265 and ZMIZ2 distinctly attenuates colorectal tumorigenesis in mice. Mechanistically, LINC00265 augments ZMIZ2 expression by acting as an endogenous sponge against several miRNAs, which directly target ZMIZ2 expression. Moreover, ZMIZ2 recruits the enzyme USP7, which deubiquitylates and stabilizes β-catenin, thereby facilitating colorectal tumorigenesis. In addition, β-catenin mediates LINC00265 and ZMIZ2 oncogenic phenotypes. Taken together, the LINC00265-ZMIZ2-β-catenin signaling axis plays a critical role in the colorectal tumorigenesis, which may be a potential therapeutic target.

Introduction

Colorectal cancer (CRC) imposes a pronounced cause of morbidity and mortality worldwide, and its pathogenesis is heterogeneous [1]. CRC risk is attributed to heritable factors, others such as inflammatory bowel disease and an unhealthy lifestyle and diet, which exacerbates CRC incidence [2]. Oncogenic mutations in KRAS lead to deregulation of several effector pathways, like phosphatidylinositol 3-kinase (PI3K) signaling, which control cell proliferation and survival, thus promoting colorectal tumorigenesis [3–5].

The WNT/β-catenin signaling is highly activated in CRC [5, 6]. Without WNT stimulation, cytoplasmic β-catenin is degraded by the destruction complex including adenomatous polyposis coli (APC), Axin, glycogen synthase kinase (GSK)-3, casein kinase Iα (CKIα) and the E3-ubiquitin ligase β-TrCP. β-catenin phosphorylation by GSK-3 and CKIα facilitates β-TrCP-mediated β-catenin ubiquitination and degradation in the proteasome [6, 7]. Upon WNT activation, WNT binds to the receptor Frizzled and associates AXIN with LRP5/6. This allows the destruction complex to fall apart and β-catenin to be stabilized. Subsequently, β-catenin translocates to the nucleus where it binds to the TCF1/LEF1 transcription factors and activates its transcriptional program [6, 7]. Genetic mutations in the core components of Wnt/β-catenin signaling, like *APC* mutation, lead to WNT signaling hyperactivation to drive CRC occurrence [6, 7]. However, the concrete mechanism of colorectal tumorigenesis is remained to be elucidated.

Long noncoding RNA (lncRNA) is now defined as the long RNA transcripts with more than 200 nucleotides lacking protein encoding potential [8, 9]. Lots of evidence indicates that lncRNA harbors critical impacts in regulating gene expression at levels of chromatin modification, transcriptional and posttranscriptional regulation [8]. Many lncRNAs have

Edited by J.M. Hardwick

Supplementary information The online version of this article (https://doi.org/10.1038/s41418-019-0417-3) contains supplementary material, which is available to authorized users.

✉ Youjun Li
liy7@whu.edu.cn

[1] Hubei Key Laboratory of Cell Homeostasis, College of Life Sciences, Wuhan University, 430072 Wuhan, China

[2] Medical Research Institute, School of Medicine, Wuhan University, 430071 Wuhan, China

[3] Department of Gastroenterology, Zhongnan Hospital of Wuhan University School of Medicine, 430071 Wuhan, China

[4] Hubei Clinical Center and Key Laboratory for Intestinal and Colorectal Diseases, 430071 Wuhan, China

been identified to affect tumorigenesis. HOTAIR was one of the first lncRNAs reported to interact with polycomb repressive complex 2 subunits that regulated chromatin state, and promoted invasion and metastasis of breast and colon cancer [10]. Long noncoding RNA UPAT was reported to interact with and stabilize the epigenetic factor UHRF1 by interfering with its β-transducin repeat-containing protein-mediated ubiquitination to promote colon tumorigenesis [11]. LncGata6 was shown to recruit the NURF complex onto the Ehf promoter to induce its transcription, which promotes Lgr4/5 expression to enhance Wnt signaling activation and maintain stemness of intestinal stem cells and promote tumorigenesis [12]. LINC00265 is located on human chromosome 7p14.1 and there is no mouse ortholog gene. Recently, LINC00265 was shown to be upregulated in CRC and associated with poor prognosis. Its deficiency decreases cell viability and glycolysis through directly binding to and negatively regulating miR-216b-5p, while supplementation with ectopic miR-216b-5p significantly compromises the oncogenic activities of LINC00265 in CRC cells [13]. AML patients with higher serum LINC00265 expression suffer poorer overall survival. LINC00265 contributes to AML migration and invasion via modulation of PI3K/AKT signaling [14].

ZMIZ1 and ZMIZ2 are PIAS-like proteins that are originally recognized as androgen receptor interacting proteins [15–17]. They both share a zinc-binding SP-RING/MIZ domain, which is conserved and mediates the interaction between Msx2 and PIASxβ. They also contain a C-terminal transactivation domain that augments the AR-mediated transcription [15]. ZMIZ1 has been shown to interact with P53 as a transcriptional activator [18] and also cooperates with NOTCH1 to enhance c-Myc-driven T-ALL [19]. ZMIZ2 is a nuclear protein that most highly expresses in testis [15] and it accelerates β-catenin-mediated transcription and augments prostate cancer cell growth [20]. However, the specific mechanism is unclear.

In this study, in a systematic screen, LINC00265 is upregulated and highly correlated with poor clinical outcome in human patients with CRC. LINC00265 acts as an miRNA sponge to enhance ZMIZ2 expression. Furthermore, ZMIZ2 recruits USP7 to stabilize β-catenin, which facilitates colorectal tumorigenesis. Altogether, the LINC00265-ZMIZ2-β-catenin axis is indispensable for colorectal tumorigenesis.

Results

LINC00265 upregulation is predictive of poor clinical outcomes in human CRCs

In order to find the hyperactive gene in colorectal tumorigenesis, we analyzed gene expression in CRC from TCGA database [21]. Interestingly, 2585 genes were upregulated in all CRCs and 2106 genes were highly activated in CRCs from matched normal and CRC tissues. In all, 1932 of the above genes were upregulated in both groups with the mRNA abundance from 1512 of these genes being >10 by RNA-SeqV2 analysis. Since survival rate is the most important parameter in patients prognosis, 302 such genes were noted as being significantly negative correlated ($P < 0.05$) between survival and mRNA level. Next, 268 genes were identified to be essential genes in CRC cell lines from Project Achilles [22]. Intriguingly, LINC00265, the unique lncRNA, was among these genes (Fig. 1a). Therefore, LNC00265 was chosen for further study.

To investigate the clinical significance of LINC00265 in CRC, TCGA, GSE25070 and CCLE databases were checked. LINC00265 was upregulated in virtually all tumors from matched normal and CRC tissues (Fig. 1b and Supplementary Fig. S1a, b). In CRC patients, those with tumor stage III/IV had high expression (Fig. 1c). Finally, patients with high expression usually had significantly poor survival (Fig. 1d). These findings suggest that LINC00265 overexpression is tightly related to the CRC occurrence and may contribute to the other clinical character in CRC.

LINC00265 inhibition retards CRC development

To evaluate the effects of LINC00265 on CRC development, we first identified LINC00265 to be an essential gene in colorectal cell lines from the dataset of Project Achilles (Supplementary Fig. S2) [22]. Then shRNA-mediated inhibition of LINC00265 significantly retarded cell growth in vitro and in vivo xenograft growth, while it had no effect in two tested nontransformed cells (Fig. 2a–e). Altogether these results indicate that LINC00265 is essential for CRC growth.

LINC00265 increases ZMIZ2 expression as a miRNA sponge

To illustrate the specific mechanism that LINC00265 exacerbates the CRC development, correlation analysis between LINC00265 and other gene expression was conducted in CRC from TCGA. Interestingly, among 25,000 genes, ZMIZ2 expression was extremely positively related with LINC00265 in all CRC tissues (Fig. 3a–e).

Then, we examined how LINC00265 regulated ZMIZ2 expression. LINC00265 inhibition decreased ZMIZ2 in both RNA and protein levels; in the meantime, inhibition of Dicer1, which is an essential miRNA processing enzyme, largely rescued and enhanced ZMIZ2 expression (Fig. 3f, g). We hypothesized that LINC00265 regulated ZMIZ2 through miRNAs. As miRNAs are located mostly in cytoplasm, qPCR assay implicated that LINC00265 accounted for more than 60% in cytoplasm in HCT116, SW480 and RKO, and almost

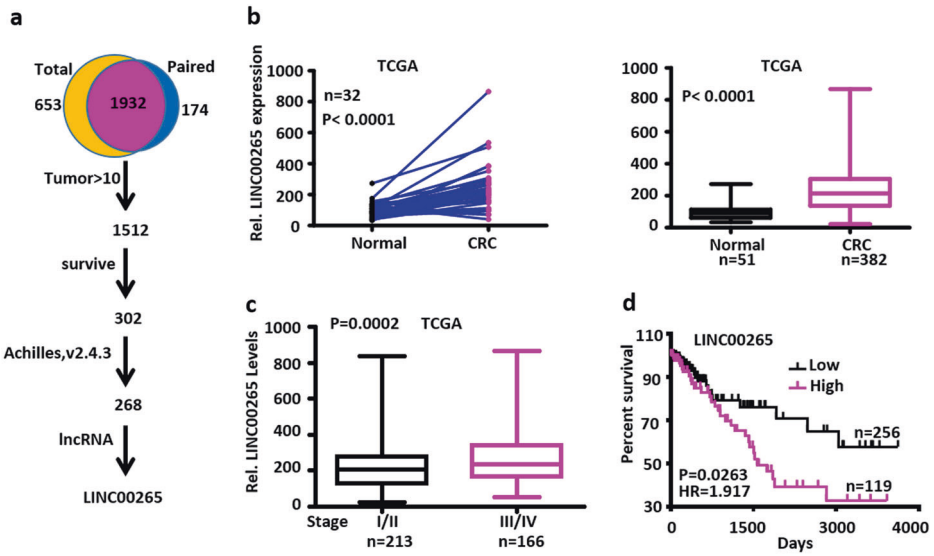

Fig. 1 LINC00265 upregulation is predictive of poor clinical outcomes in human CRCs. **a** Summary of bioinformatic screening results in the CRCs from TCGA database. Among 2,0531 genes, 2585 genes were upregulated in all CRCs and 2106 ones were highly activated in CRCs from matched normal and CRC tissues. A total of 1932 of the above genes were upregulated in both groups with the mRNA abundance from 1512 of these genes being >10 by RNA-SeqV2 analysis. In all, 302 such genes were noted as being significantly negative correlated ($P < 0.05$) between survival and mRNA level. In all, 268 of these genes were identified to be essential genes in CRC cell lines from Project Achilles. Among these, only one lncRNA, LINC00265, was selected. **b** Relative RNA levels of LINC00265 in normal and CRC tissues from TCGA. **c** Association of LINC00265 expression with clinical stages in CRC patients from TCGA dataset. **d** Survival of human CRC patients from TCGA dataset with LINC00265 expression high versus low. *P* values are indicated. **b**, **c** Significance was performed using Wilcoxon signed rank test. The horizontal lines in the box plots represent the median, the boxes represent the interquartile range, and the whiskers represent the minimal and maximal values

half in DLD1 in both nucleus and cytoplasm (Fig. 3h). Next, we sought for potential miRNAs that target LINC00265 and ZMIZ2. These indicated that only four miRNAs, miR-30c-2-3p, miR-130-3p, miR-324-3p and miR-375, were inversely correlated and harbored more than one binding site with both LINC00265 and ZMIZ2 (Fig. 3i). Q-PCR and immunoblot showed that these four miRNAs all substantially reduced ZMIZ2 expression in HCT116 and SW480 cells (Fig. 3j, k). Co-IP using the antibody AGO-2 to precipitate RNAs associated with the RNA-induced Silencing Complex (RISC) indicated that the above target RNAs were significantly enriched with LINC00265 and ZMIZ2 (Fig. 3l). Moreover, ectopic miRNA expression abrogated the activity of LINC00265 and ZMIZ2-3′UTR in dual luciferase reporter assays, while mutations of the LINC00265 and ZMIZ2 binding sites exposed no effects in luciferase activity in both HCT116 and SW480 cells. Above all, these data elucidate that LINC00265 enhances ZMIZ2 expression as a miRNA sponge.

ZMIZ2 is upregulated and predictive of poor clinical outcome

To investigate the role of ZMIZ2 in CRC development, we analyzed the expression of ZMIZ2 in different databases. ZMIZ2 was significantly upregulated in all CRC tissues (Fig. 4a–c). The protein level of ZMIZ2 in CRC tissues also exceeded adjacent normal ones (Fig. 4d and Supplementary Fig. S3a). In patients with CRC, those with stage III/IV had significantly higher ZMIZ2 expression than those with stage I/II (Supplementary Fig. S3b). In addition, the patients with CRC who survived longer were accompanied with lower ZMIZ2 expression (Fig. 4e).

ZMIZ2 inhibition retards CRC tumor growth

Then, we evaluated whether ZMIZ2 modulated CRC growth. ZMIZ2 knockdown significantly inhibited CRC cell growth from the database of the Project Achilles (Supplementary Fig. S3c). ShRNA-mediated inhibition of ZMIZ2 retarded cell growth in vitro (Supplementary Fig. S3d) and in vivo (Fig. 4f–i) xenograft growth, while overexpression of shRNA-resistant ZMIZ2 largely rescued these defects.

Next, we explored whether LINC00265's oncogenic effects were ZMIZ2 dependent. Depletion of LINC00265 blocked CRC cell growth, while ectopic ZMIZ2 expression abundantly reversed the tumor phenotype in vivo and in vitro (Fig. 4j−m and Supplementary Fig. S3e). Altogether, these data suggest that ZMIZ2 increases CRC development and the oncogenic phenotypes of LINC00265 are partially mediated by ZMIZ2.

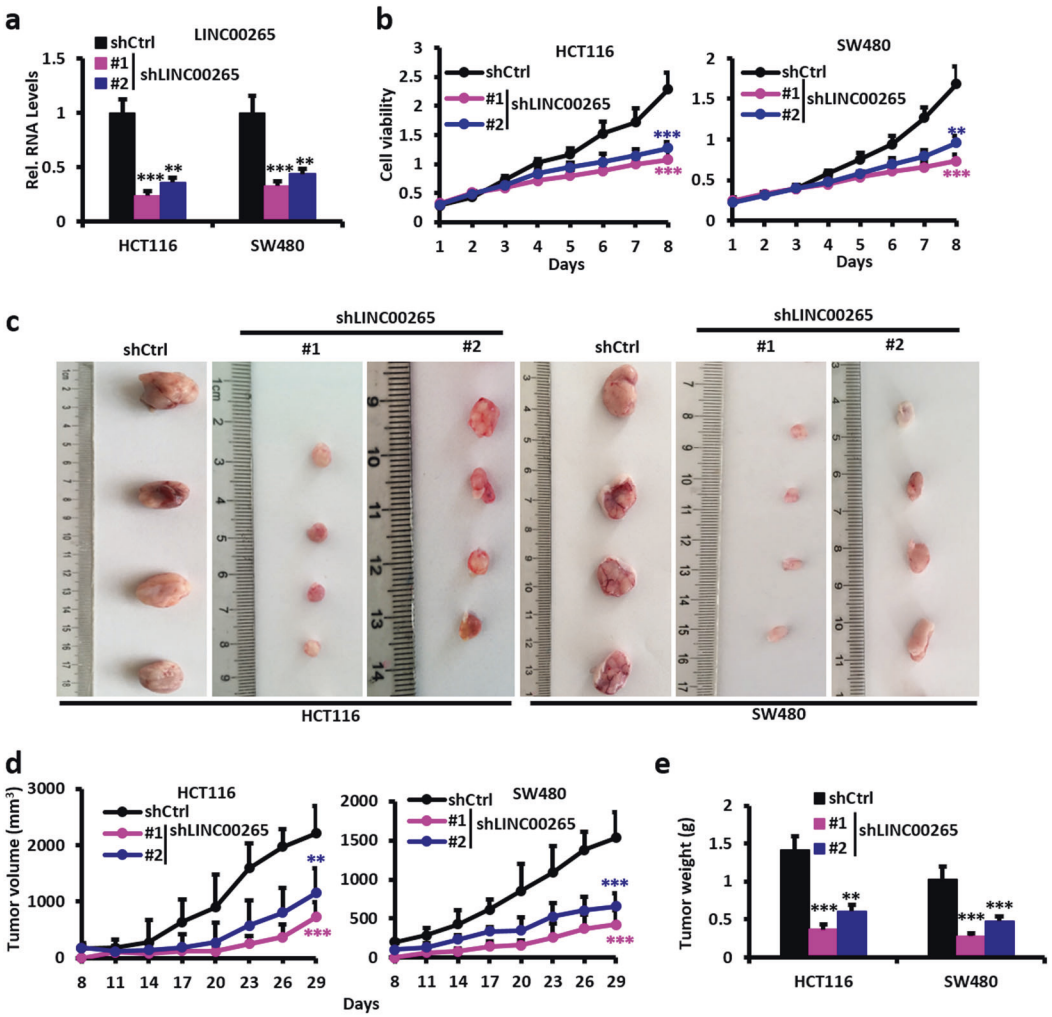

Fig. 2 LINC00265 inhibition retards CRC development. **a** Relative RNA levels were determined by qRT-PCR with LINC00265 depletion CRC HCT116 and SW480 cells. **b** MTT assays showed relative absorbance of indicated cells. **c**–**e** Xenograft growth in nude mice ($n = 5$). Tumor photographs (**c**), tumor growth curve (**d**), and tumor weight (**e**). Data were presented as mean ± SD. $^{**}P < 0.01$, $^{***}P < 0.001$

LINC00265 enhances β-catenin signaling via ZMIZ2

To identify the signaling pathway that LINC00265 participates in, we conducted gene ontology (GO) analysis on the significantly changed genes associated with LINC00265 in CRC from TCGA. We found that most of the related genes are involved in microtube, adherens junction and WNT/β-catenin signaling pathway (Fig. 5a). Since WNT signaling plays a significant role in CRC and ZMIZ2 has been reported to interact with β-catenin [11, 20], we hypothesized that LINC00265 regulates β-catenin through ZMIZ2. Heatmaps indicated that LINC00265 and ZMIZ2 were positively correlated with many β-catenin target genes (Fig. 5b and Supplementary Fig. S4a). Inhibition of LINC00265 depressed β-catenin expression and downstream target genes in CRC HCT116 and SW480 cells (Fig. 5c and Supplementary Fig. S4b), while ectopic ZMIZ2 expression largely rescued these defects (Fig. 5d and Supplementary Fig. S4c, d). Consistently, ZMIZ2 inhibition aborted β-catenin expression (Fig. 5e and Supplementary Fig. S4e, f).

Next, we investigated whether ZMIZ2 interacted with β-catenin dependent on LINC00265. Co-IP displayed that after suppressing LINC00265, the interaction between ZMIZ2 and β-catenin was attenuated in HCT116 and SW480 (Fig. 5f, g and Supplementary Fig. S4g, h). Cycloheximide (CHX) assay indicated that ZMIZ2 inhibition greatly prolonged β-catenin turnover (Fig. 5h and Supplementary Fig. S4i).

Then NH_4Cl, MG132, and 3-MA were used to inhibit lysosomal, proteasomal, and autophagocytic pathways of protein degradation, respectively. We found that only MG132 treatment stabilized β-catenin protein level (Supplementary Figure S4j); in other words, ZMIZ2 stabilized β-catenin via proteasome pathway.

Then, we evaluated whether ZMIZ2 stabilized β-catenin through deubiquitination. As assumed, ectopic ZMIZ2

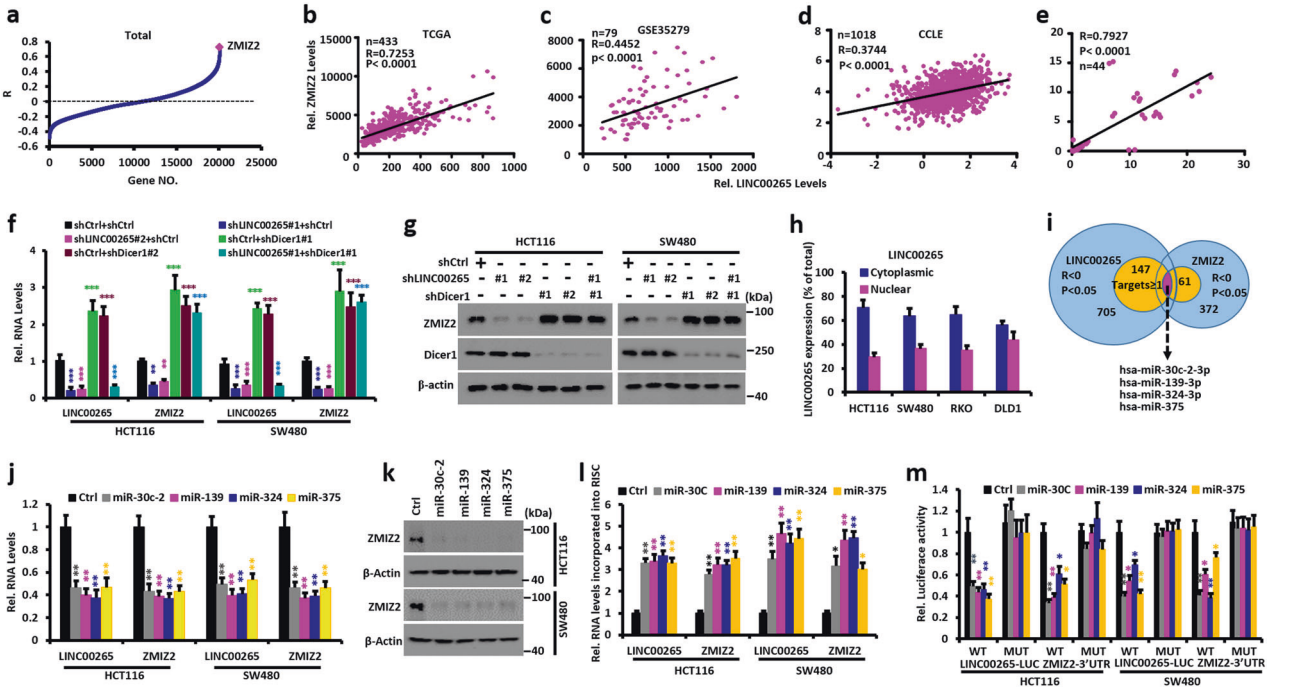

Fig. 3 LINC00265 upregulates ZMIZ2 expression as an miRNA sponge. **a** The correlation between the expression of LINC00265 and genes in the CRCs from TCGA dataset. **b**, **e** The correlation between the expression of LINC00265 and ZMIZ2 in the CRCs from TCGA dataset (**b**), GSE35279 (**c**), CCLE (**d**) and clinical patients with CRC (**e**). Each point is an individual sample. R, Spearman correlation coefficient. **f** Relative RNA levels of LINC00265 and ZMIZ2 in the indicated stable cells. **g** The protein level of ZMIZ2 in the indicated stable cells. **h** Relative LINC00265 expression of cytoplasm and nucleus in different CRC cells. **i** Common miRNAs targeting LINC00265 and ZMIZ2. **j**, **k** Relative RNA (**j**) and protein (**k**) levels of LINC00265 and ZMIZ2 in the indicated stable cells. **l** RT-qPCR analysis was performed to detect RNA levels of LINC00265 and ZMIZ2 incorporated into RISC derived from miRNAs overexpression. **m** Luciferase activity of the reporters containing indicated vectors was determined after cotransfection with Ctrl, miR-30c, miR-139, miR-324 or miR-375. Data were presented as mean ± SD. $*P < 0.05$, $**P < 0.01$, $***P < 0.001$

expression reduced the polyubiquitination of β-catenin and ZMIZ2 inhibition had the opposite effect (Fig. 5i, j). To identify the type of β-catenin deubiquitination mediated by ZMIZ2, we used several vectors expressing HA-tagged mutant Ubiquitin (K6O, K11O, K27O, K29O, K33O, K48O and K63O), which contained substitutions of arginine for all lysine resides except the lysine at this position, respectively [23]. Deubiquitination of β-catenin was detected mostly in the presence of wild type (WT) and K48O, but a little in K6O and K33O were also identified (Fig. 5k). Altogether, LINC00265 enhances β-catenin signaling via ZMIZ2, and ZMIZ2 stabilizes β-catenin mainly through K48-linked deubiquitination.

ZMIZ2 recruits USP7 to stabilize β-catenin

To evaluate which deubiquitinase (DUB) mediates β-catenin stability, firefly luciferase fused to the N terminus of β-catenin (β-catenin-Luc) was used as a reporter of β-catenin stability [24]. Eighteen DUBs were tested and only USP7, which is major localized in nucleus, could largely improve the β-catenin protein levels in the control cell and decrease the luciferase activity upon ZMIZ2 inhibition (Fig. 6a–c). Ectopic USP7 expression stabilized β-catenin, while USP7 catalytic inactive mutant (C223A) had no effect. Inversely, USP7 inhibition got the opposite effect and it could be reversed by WT rather USP7 mutant expression (Supplementary Fig. S5a−d). These all suggest that ZMIZ2 stabilizes β-catenin through USP7.

Then, we examined how USP7 participated in ZMIZ2-mediated stabilization of β-catenin. Ectopic USP7 expression largely prolonged the half-life of β-catenin while ZMIZ2 repression impaired this effect (Fig. 6d and Supplementary Fig. S5e). Conversely, USP7 inhibition shortened the turnover of β-catenin and ectopic ZMIZ2 expression could not rescue this defect (Fig. 6e and Supplementary Fig. S5f). Co-IP assay indicated that ZMIZ2, USP7 and β-catenin were all interacting with each other in the nucleus (Fig. 6f, g and Supplementary Fig. S5g). We then mapped the interaction region and found that the N-terminal of ZMIZ2 and MATH domain of USP7 were required to interact with each other (Supplementary Fig. S5h, i). Moreover, depletion of ZMIZ2 impaired the interaction between USP7 and β-catenin, but USP7 repression did not affect the interaction between ZMIZ2 and β-catenin (Fig. 6h, i), implicating that ZMIZ2 mediates the interaction between USP7 and β-catenin.

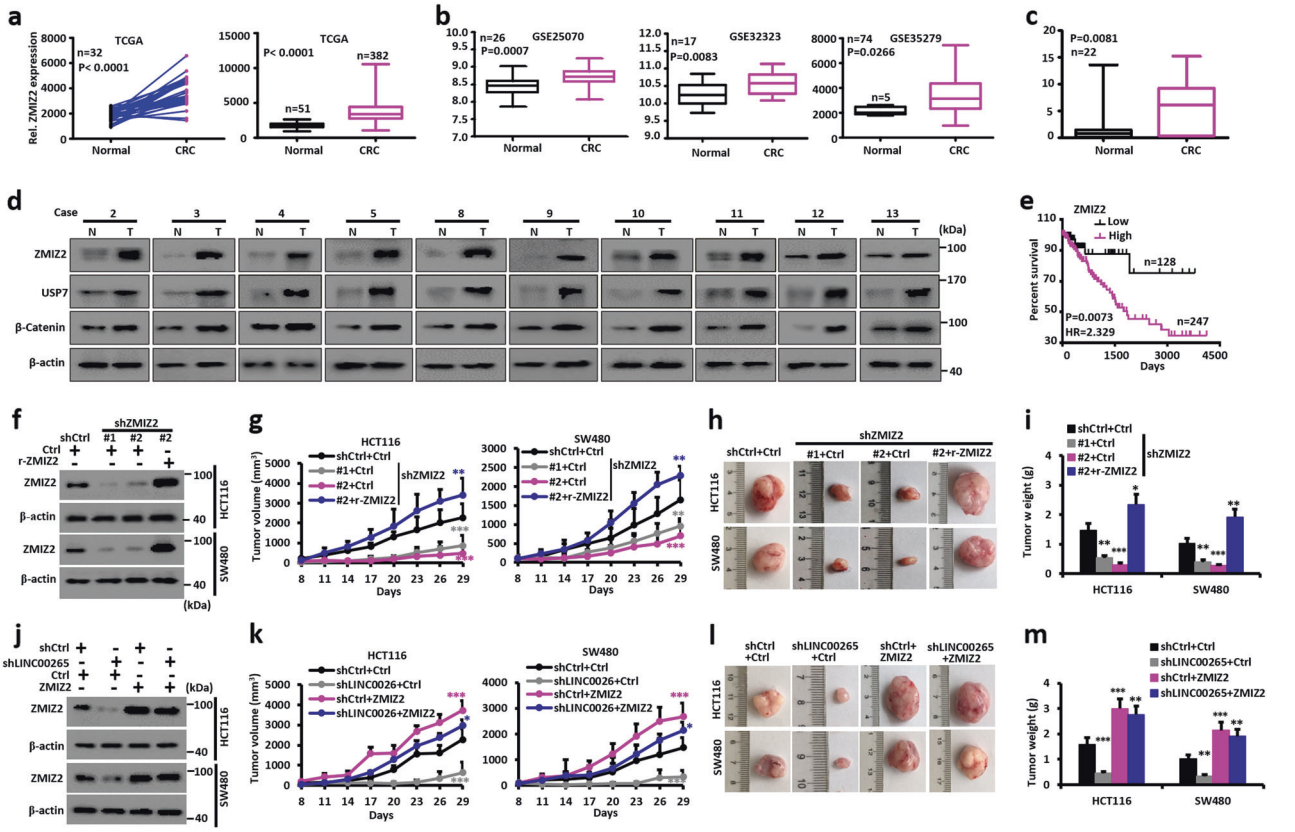

Fig. 4 ZMIZ2 upregulation is predictive of poor clinical outcome. **a** Relative ZMIZ2 mRNA levels in paired (left) and nonpaired (right) normal and CRC tissues from TCGA dataset. **b** Relative ZMIZ2 mRNA levels in normal and CRC tissues from GSE25070 (left), GSE32323 (middle) and GSE35279 (right). **c**, **d** Relative RNA levels (**c**) and protein expression (**d**) of ZMIZ2 in the tumor tissues of CRC patients. **e** Survival of human patients with CRC from TCGA dataset, with high versus low ZMIZ2 expression. **f** Western blot analysis of ZMIZ2 protein level in the indicated stable cells. **g**–**i** Xenograft growth in nude mice. Tumor growth curve after injecting the indicated cells (**g**) and photographs of tumors (**h**) and tumor weight (**i**) from the indicated cells were determined. **j** Western blot analysis of ZMIZ2 protein level in the indicated stable cells. **k**–**m** Tumor volume (**k**), tumor photos (**l**) and tumor weight (**m**) of xenograft mice injected with indicated cells. **a**: right, **b**, **c** Significance was performed using Wilcoxon signed rank test. The horizontal lines in the box plots represent the median, the boxes represent the interquartile range, and the whiskers represent the minimal and maximal values. Data were presented as mean ± SD. $^{*}P < 0.05$, $^{**}P < 0.01$, $^{***}P < 0.001$

In addition, we detected whether USP7 deubiquitinated β-catenin. Ectopic USP7 expression reduced the polyubiquitination of β-catenin and ZMIZ2 inhibition could reverse this effect (Fig. 6j). Similarly, USP7 inhibition enhanced the ubiquitination of β-catenin; at the same time, ectopic ZMIZ2 expression did not affect this effect (Supplementary Fig. S5j). Collectively, these data indicate that ZMIZ2 recruits USP7 to deubiquitinate and stabilize β-catenin.

β-catenin mediates LINC00265 and ZMIZ2 oncogenic phenotypes

Then, we evaluated whether LINC00265 and ZMIZ2 promoted CRC dependent on β-catenin. LINC00265 and ZMIZ2 inhibition severely retarded colon cell growth in MTT assay and xenograft growth in mice and reduced the expression of β-catenin target genes, while β-catenin overexpression enormously rescued these defects (Fig. 7a–h and Supplementary Fig. S6a–f). Conversely, HCT116 and SW480 cells with ZMIZ2 upregulation grew more rapidly than their control counterparts both in vitro and in vivo, and these effects were largely reversed by β-catenin abrogation (Fig. 7i–l and Supplementary Fig. S6g–i). These results imply that β-catenin mediates LINC00265 and ZMIZ2 oncogenic phenotypes.

ZMIZ2 repression attenuates spontaneous and chemical-induced tumorigenesis in mice

To elaborate the effects of ZMIZ2 in colorectal tumorigenesis, we exploited an established CRC model [24, 25]. Female mice were injected intraperitoneally with DNA-methylation agent AOM, followed by three rounds of DSS treatment. During this period, concentrated adenoviruses containing ZMIZ2 shRNAs were injected intraperitoneally and mice were sacrificed after 120 days (Supplementary

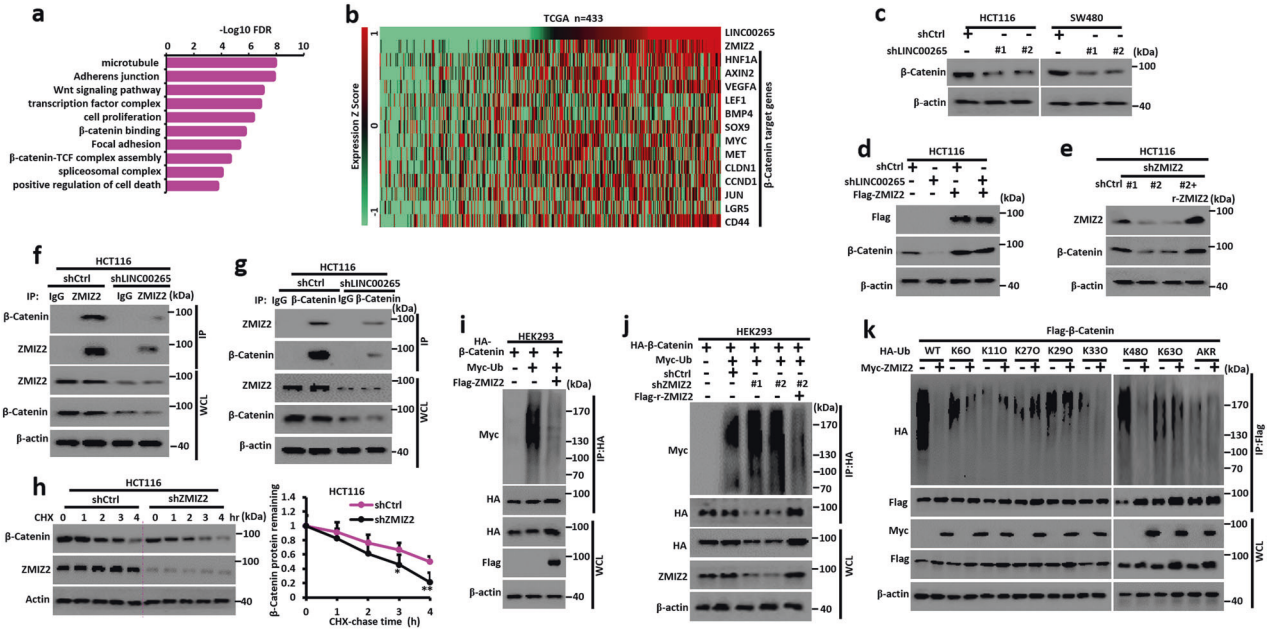

Fig. 5 LINC00265 increases β-catenin signaling via ZMIZ2. **a** Gene ontology (GO) analysis of the significantly altered genes associated with LINC00265 in the TCGA dataset. **b** Heatmap shows the relative RNA expression of β-catenin target genes that LINC00265 is positively associated with CRCs from TCGA dataset. **c** Western blot indicated the β-catenin expression in LINC00265 depletion HCT116 and SW480 cells. **d**, **e** The protein level of β-catenin and ZMIZ2 in the indicated stable cells. **f**, **g** Depletion of LINC00265 reduced the interaction between ZMIZ2 and β-catenin. HCT116 cells were cotransfected with indicated vectors. IP and IB with indicated antibodies were performed. **h** ZMIZ2 affects β-catenin protein turnover. HCT116 cells were transfected with indicated vectors. After cells were treated with CHX (50 μg/ml) for the indicated time, expression of β-catenin and ZMIZ2 was analyzed by western blotting (left); the intensity of β-catenin expression for each time point was quantified by densitometry with β-actin as a normalizer (right). **i**, **j** Ectopic ZMIZ2 expression increases β-catenin deubiquitination (**i**) and depletion of ZMIZ2 decreased β-catenin deubiquitination (**j**). HEK293 cells were transfected with Myc-ubiquitin (Ub), HA-β-catenin, Flag-ZMIZ2 or ZMIZ2 shRNAs. IP and IB were performed with the indicated antibodies. **k** ZMIZ2 promotes K6-, K33- and K48-linked deubiquitination of β-catenin. HEK293 cells were cotransfected with Flag-β-catenin, ZMIZ2 and HA-Ub or its mutants as indicated

Fig. S7a). Western blot indicated that ZMIZ2 expression was gradually elevated during CRC development (Fig. 8a). At day 120, ZIMZ2 was expressed much higher than day 60 in AOM/DSS-induced CRC and there were nearly no changes in normal mice (Fig. 8b).

In the AOM/DSS-induced CRC model, mice containing ZMIZ2 shRNAs illustrated fewer tumors per colon and a smaller tumor size (Fig. 8c–e). Western blot indicated ZMIZ2 was indeed knocked down in colon tissues (Fig. 8f) and the expression of β-catenin target genes was also downregulated (Supplementary Fig. S7b).

APC is a critical constituent in WNT/β-catenin pathway and $APC^{Min/+}$ is a widely used colon cancer model for sporadic CRC [25, 26]. Likewise, ZMIZ2 expressed higher in $APC^{Min/+}$ mice (Supplementary Fig. S7c), so we tested whether ZMIZ2 functions in the spontaneous CRC development. Adenoviruses with ZMIZ2 shRNAs were injected six times weekly from week 4, and mice were sacrificed around day 100 (Supplementary Fig. S7d). In $APC^{Min/+}$ spontaneous CRC model, mice containing ZMIZ2 shRNAs illustrated fewer tumors, a smaller tumor size and lower expression of β-catenin target genes in the colon and small intestine (Fig. 8g, h, Supplementary Fig. S7e–k). Collectively, these data demonstrate that ZMIZ2 repression attenuates spontaneous and chemical-induced CRC development in mice.

β-catenin transcriptionally activates LINC00265

Our results showed that LINC00265 was significantly upregulated in CRC. Because activation of β-catenin signaling pathway is pivotal during colorectal tumorigenesis [5–7], we tested whether β-catenin signaling was responsible for LINC00265 upregulation in CRC. To this end, we analyzed the putative transcription factors binding to the LINC00265 promoter region (−10 to +10 kb) in the motifmap website. This revealed LEF1/TCF1 as the top candidate and these sites were largely conserved (Supplementary Fig. S8a). Ectopic β-catenin expression upregulated LINC00265 RNA level (Supplementary Fig. S8b, c) and depletion of β-catenin had the opposite effect (Supplementary Fig. S8d, e).

We next detected whether β-catenin directly transactivates LINC00265 using chromatin immunoprecipitation (CHIP) assays. The results showed that β-catenin occupied

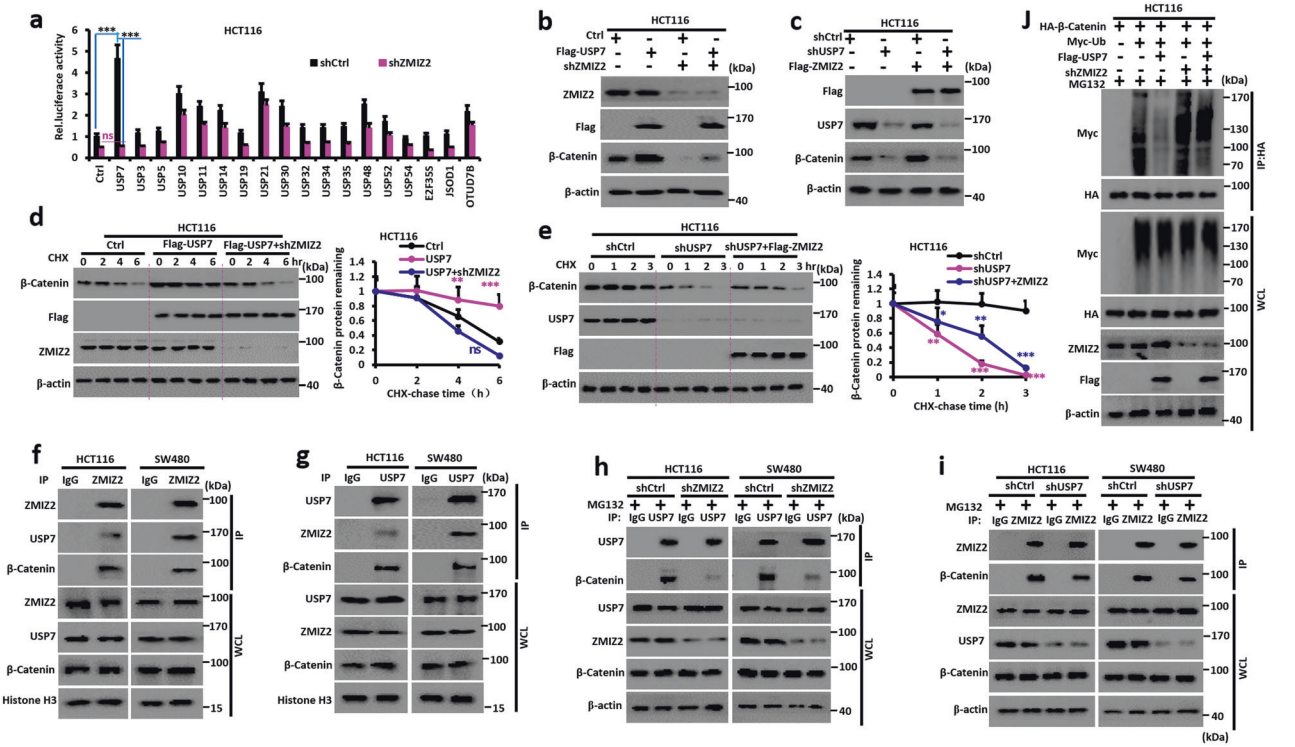

Fig. 6 ZMIZ2 recruits USP7 to deubiquitinate and stabilize β-catenin. **a** Screening for the deubiquitinating enzymes of β-catenin. The indicated DUBs were overexpressed in HCT116 and used for luciferase assay. **b**, **c** Western blot analysis of protein expression in the indicated stable cells. **d**, **e** USP7 prolongs β-catenin protein turnover. HCT116 cells were transfected with indicated vectors. After cells were treated with CHX (50 μg/ml) for the indicated time, expression of β-catenin and ZMIZ2 was analyzed by western blotting (**d** and **e**, left); the intensity of β-catenin expression for each time point was quantified by densitometry with β-actin as a normalizer (**d** and **e**, right). **f**, **g** ZMIZ2 interacts with USP7 and β-catenin. HCT116 and SW480 cells were transfected with indicated vectors. IP and IB with indicated antibodies were performed. **h**, **i** ZMIZ2 mediates the interaction between USP7 and β-catenin. HCT116 and SW480 were transfected with indicated vectors. IP and IB with indicated antibodies. **j** USP7 deubiquitinates β-Catenin. $^{*}P < 0.05$, $^{**}P < 0.01$, $^{***}P < 0.001$

the promoters of LINC00265 in HCT116 and SW480 cells (Supplementary Fig. S8f). Thus, β-catenin transcriptionally activates LINC00265.

Discussion

lncRNAs are recognized to be fundamental for eukaryotes and indispensable for cancer progression [8, 9]. With the characteristic of noninvasiveness and stable in body fluids, lncRNA has become a promising and sensitive biomarker for cancer diagnosis and prognosis [9]. In this study, we demonstrate that LINC00265 is significantly upregulated in CRCs. LINC00265 acts as an miRNA sponge to upregulate ZMIZ2. ZMIZ2 mediates the interaction between USP7 and β-catenin to deubiquitinate and stabilize β-catenin, led to colorectal tumorigenesis (Fig. 8i).

Intriguingly, LINC00265 and ZMIZ2 are extremely positively correlated and both are upregulated in human CRCs. It has been reported that linc-MD1 acted as a natural decoy for miR-133 and miR-135 to activate MAML1 and MEF2C in muscle [25]. LncARSR functions as a ceRNA for miR-34 and miR-449 to facilitate AXL and c-MET expression in renal cell carcinoma [26]. Recently, circular RNA circMTO1 was identified as a sponge of miR-9 to inhibit p21 expression and repressed HCC progression [27]. In our model, LINC00265 functions as a competing endogenous RNA of hsa-miR30-2-3p, hsa-miR-139-3p, hsa-miR-324-3p and hsa-miR-376 to stimulate ZMIZ2 expression and promote CRC development.

ZMIZ2 has been shown to interact with β-catenin and enhance β-catenin-mediated transcription in prostate cancer [20]. Our results shows that LINC00265 upregulates WNT/β-catenin signaling through ZMIZ2. ZMIZ2 stabilizes β-catenin through K6-, K33- and K48-linked deubiquitination. It is well known that K48-linked ubiquitination is associated with protein degradation, but how K6- and K33-linked ubiquitination functions in ZMIZ2-mediated β-catenin stabilization remains to be elucidated.

It was reported that USP7 promoted WNT signaling in mutant *APC*-driven CRC and RNF220 enhanced WNT signaling through USP7 deubiquitination [28, 29]. Several other DUBs such as USP2a, USP9x, USP20 and USP47

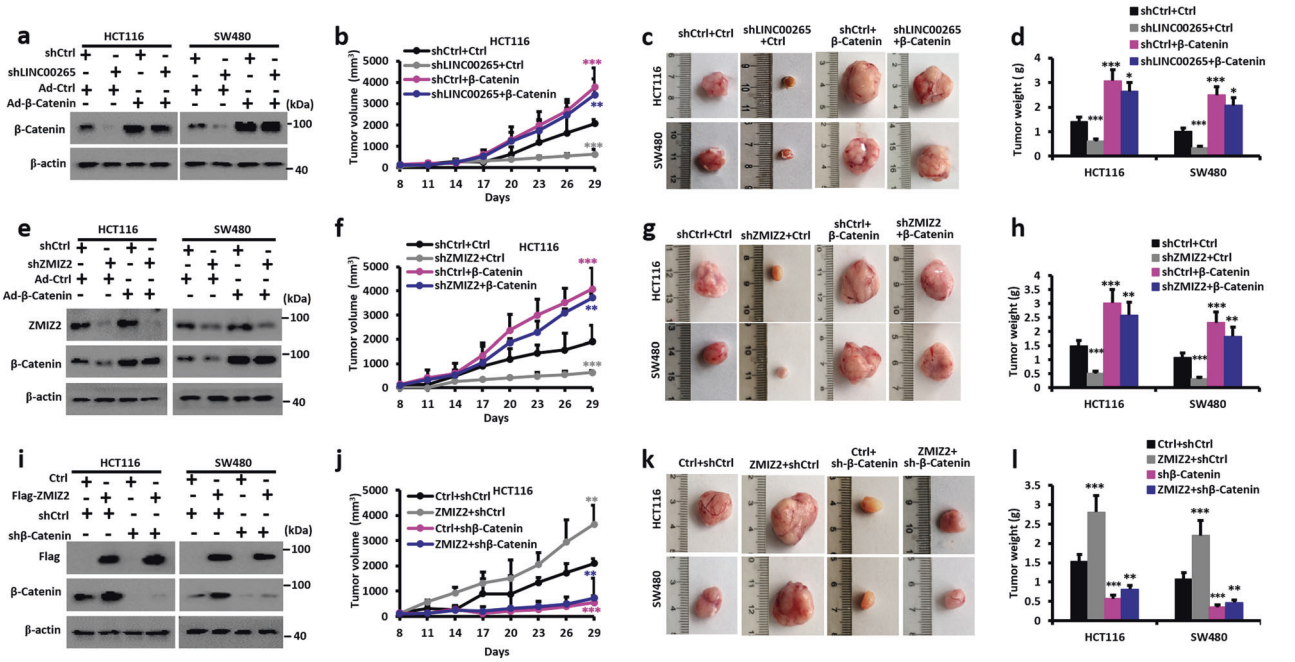

Fig. 7 β-catenin mediates LINC00265 and ZMIZ2 oncogenic phenotypes. **a**, **e**, **i** Western blot analysis in HCT116 and SW480 cells stably expressing indicated vectors with indicated antibodies. **b**–**d**, **f**–**h**, **j**–**l** Xenograft growth in nude mice. HCT116 and SW480 cells stable expressing indicated vectors were injected subcutaneously into nude mice ($n = 5$). Tumor volumes were measured every 3 days. Tumor growth curve after injecting the indicated cells (**b**, **f**, **j**), photographs of tumors (**c**, **g**, **k**) and tumor weight (**d**, **h**, **l**) from indicated cells were analyzed. Data were presented as mean ± SD. $^{*}P < 0.05$, $^{**}P < 0.01$, $^{***}P < 0.001$

also deubiquitinate β-catenin and promote tumorigenesis [30–33]. In our work, we defined that ZMIZ2 stabilized β-catenin through USP7 with luciferase reporter screen. USP7 is one of the widely characterized DUBs and is functionally significant as it is the specific deubiquitinase for P53, the major tumor suppressor in cellular process [34]. USP7 interacts with many vital proteins, such as polycomb repressor complex 1 (PRC1), histone H2A and H2B, checkpoint kinase (CHK1), phosphatase and tensin homolog (PTEN), viral protein EBNA1 and so on, and is dysregulated in cancer progression [35–37]. Thus, many trials have been devoted to identify USP7 inhibitors for treatment of cancers [38]. We defined that ZMIZ2 recruits USP7 to deubiquitinate and stabilize β-catenin.

ZMIZ2 accelerates CRC progression in spontaneous and carcinogen-induced tumor mice models through β-catenin pathway. ZMIZ2 stabilizes β-catenin to enhance its target genes expression and constitutive activation of β-catenin led to colorectal tumorigenesis. *APC* is a vital suppressor gene in WNT signaling and 45–80% CRCs were *APC* monoallelic mutant [39]. Re-establishing *APC* expression can restore normal development and differentiation in the intestinal crypt epithelium in mice with *APC*-deficient CRC. *APC* loss causes early premalignant lessons and is sensitive and prone to die [39, 40]. With $Apc^{Min/+}$ mice, ZIMZ2 repression effectively retards colon and intestine tumor growth.

In summary, a new lncRNA, LINC00265, was identified to upregulate ZIMZ2 as an miRNA sponge. ZMIZ2 recruits USP7 to deubiquitinate and stabilize β-catenin. LINC00265 and ZMIZ2 enhance β-catenin signaling and promote CRC progression. Altogether, these findings offer a new link between LINC00265 and WNT/β-catenin-driven CRC development and provide a promising therapy target.

Materials and methods

Clinical human CRC specimens

CRC samples were used as previously described [24]. Written informed consent was obtained from all patients at the Union Hospital in Wuhan, China. The studies were conducted in accordance with Declaration of Helsinki and approved by the review board of Wuhan University. The diagnoses of all samples were confirmed by histological review.

Cell culture and reagents

Human embryonic kidney HEK293 cells were obtained from American Type Culture Collection (Rockville, MD, USA) while human colon cancer-derived cell lines HCT116, SW480, RKO and DLD1 were obtained from China Center for Type Culture Collection (Wuhan, China).

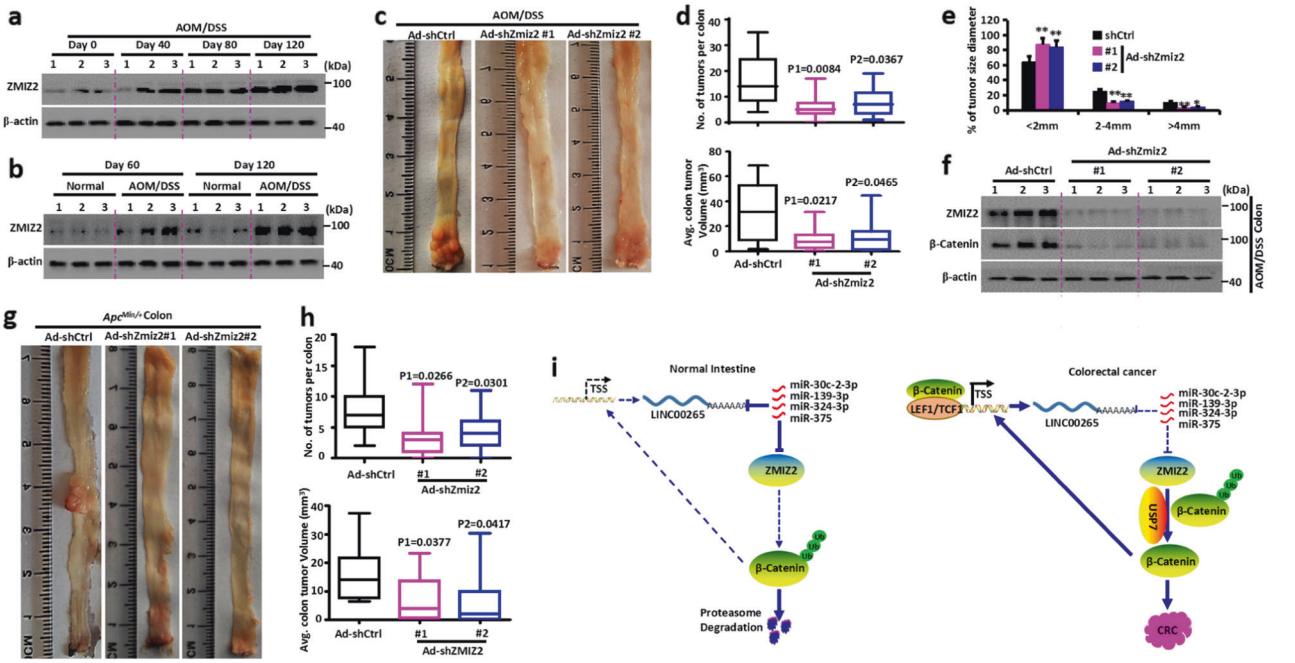

Fig. 8 Depletion of ZMIZ2 attenuates spontaneous and chemical-induced tumorigenesis in mice. **a**, **b** Western blot analysis of ZMIZ2 expression during AOM/DSS-induced CRC. **c** Images of colon tumors of mice with indicated adenovirus injection 120 days after AOM/DSS treatment. **d**, **e** Colon tumor number (**d**, top), average volume (**d**, bottom) and size (**e**) in mice from (**c**). **f** Western blot analysis of ZMIZ2 and β-catenin collected in mice from (**c**). Each lane represents an individual mice. **g** Images of colon tumors of $Apc^{Min/+}$ mice with indicated adenovirus injection. **h** Colon tumor number (**h**, top), average volume (**h**, bottom) in mice from (**g**). **i** Schematic summary. β-Catenin upregulates LINC00265 expression. LINC00265 acts as an miRNA sponge to enhance ZMIZ2 expression. ZMIZ2 recruits USP7 to deubiquitinate and stabilize β-catenin led to colorectal tumorigenesis. **d**, **h** Significance was performed using Wilcoxon signed rank test. The horizontal lines in the box plots represent the median, the boxes represent the interquartile range, and the whiskers represent the minimal and maximal values. Data were presented as mean ± SD. $^{*}P < 0.05$, $^{**}P < 0.01$

All cells, regularly authenticated by short tandem repeat analysis and tested for absence of *Mycoplasma* contamination, were used within five passages after thawing and cultured as previously described. Cycloheximide (R750107), proteasome inhibitor MG132 (M8699), and autophagy inhibitor 3-methyladenine (3-MA) (M9281) were purchased from Sigma-Aldrich. Antibodies used in this study are listed in Supplementary Table S1.

Plasmids and stable cell lines

The human ZMIZ2, USP7 and β-catenin were amplified and cloned into pHAGE-CMV-MCS-PGK-3×Flag and pCMV-HA vectors. Mutations in the USP7 C223S sequences were generated by overlap extension PCR. Short hairpin RNAs to inhibit ZMIZ2 and β-catenin were designed and synthesized by GENEWIZ (Souzhou, China). The latter were annealed and then inserted into pLKO.1-puro vector. The β-catenin-luciferase vector was generated by cloning the human β-catenin coding sequences to the luciferase gene tail of pcDNA3.1(+)-5′flag Luc. Adenovirus vector was obtained from Yan Wang (College of Life Science, Wuhan University). Primers used in this study are listed in Supplementary Table S2. Transfection and the establishment of stable cell lines were performed as previously described [23]. Cell viability was measured by MTT assay according to the manufacturer's instructions (Promega, Madison, WI, USA).

Co-immunoprecipitation and immunoblot

Transfected cells were lysed in 1 ml lysis buffer (20 mM Tris (pH 7.4), 300 mM NaCl, 1% Triton, 1 mM EDTA, 10 mg/ml aprotinin, 10 mg/ml leupeptin, and 1 mM PMSF). Sepharose beads were washed three times with 1 ml lysis buffer containing 150 mM NaCl. Co-IP and immunoblot analysis were performed as described before [23].

qRT-PCR

Total RNA was isolated using Trizol (Invitrogen, Carlsbad, CA) followed by DNase (Thermo Scientific) treatment. Reverse transcription was performed with a cDNA Synthesis Kit (Promega) and qPCR were performed using SYBR Green master mix (Bio-Rad, Hercules, CA) using standard protocols. All primer sequences used are shown in Supplementary Table S2. β-actin was used as an internal control.

RNA immunoprecipitation to pull down RISC-associated RNA

RNA immunoprecipitation (RIP) was performed according to the methods previously described [41]. Briefly, 10^7 HCT116 and SW480 cells were UV irradiated and lysed with RIP buffer containing RNase Inhibitor (EO0381, Thermo Scientific) and protease inhibitor (Sigma-Aldrich) and then treated with DNase I (Thermo Scientific). The separated supernatant was incubated with 1 mg rabbit mono-antibody against Ago-2 (D2C9, Cell Signaling) or control IgG for 4 h and then added to protein G beads (Life Technology). After digestion, the precipitated RNA was purified using Trizol reagent (Life Technology) and analyzed by real-time RT-PCR using random primer.

Luciferase assay

Human ZMIZ2–3′UTR and LINC00265 binding sequences were inserted into pGL3-basic luciferase vector (Promega). Luciferase assays were performed as described previously [41].

Nuclear/cytoplasmic extract isolation

Isolation of cytoplasmic and nuclear extracts was previously described. Briefly, the collected cells were resuspended in 10.0 mM HEPES (pH7.9), then lysed, centrifuged, and the supernatant, which contained cytoplasmic fraction, was removed to new microtubes. The pellet, which contained the nuclei, was resuspended in 20 mM HEPES (pH 7.9), and stirred at 4 °C. Then the nuclear extracts were centrifuged and the supernatant was collected. The nuclear and cytoplasmic extracts were further studied by western blot. Histone H3 was used as nuclear loading controls.

Animal studies

All animal studies were approved by the Animal Care Committee of Wuhan University. For xenograft experiments, 4-week-old male BALB/c nude mice were purchased from Model Animal Research Center (Nanjing, China) and maintained in microisolator cages. Detailed procedures were described previously [41].

For AOM/DSS-induced mice model, Ad-ZMIZ2 shRNA vectors were constructed as described by Peuker et al. [39]. Briefly, ZMIZ2 shRNAs were cloned into pShuttle-CMV-LAZ. Then linearized shuttle plasmid DNA were digested with *Pme*I and *Pac*I. After that, plasmids were transfected in cells and adenoviruses were purified. For administration, female C57/B6 mice were first treated with AOM/DSS, and randomly distributed into three groups (ten mice each group). Then mice received 3×10^9 adenoviruses by weekly intraperitoneal injection from weeks 4 to 9. At day 120, mice were sacrificed and tumor burdens were evaluated.

$Apc^{Min/+}$ mice were also ordered from Model Animal Research Center (Nanjing, China). Three-week-old female $Apc^{Min/+}$ mice were randomly distributed as above. Concentrated viruses were administrated from weeks 4 to 9 and tumor burdens were analyzed on week 14.

Bioinformatics and statistics

Online softwares miRanda, miRDB, miRwalk, PICTAR5 and Targetscan were used to predict miRNA targets of LINC00265 and ZMIZ2. CRC data sets were downloaded from The Cancer Genome Atlas (TCGA) data portal. Gene expression was assessed in human CRC tissues from the TCGA RNA-seq dataset. The information of Project Achilles was downloaded from the website (https://portals.broadinstitute.org/) in which genome-wide RNAi screens were used to systematically identify essential genes across hundreds of genomically characterized cancer cell lines [22]. Experimental data were analyzed using unpaired, and paired two-tailed Student's t test, Wilcoxon signed rank test or Mann–Whitney U test, and the correlation was analyzed using a Spearman rank correlation test. Kaplan–Meier curves for survival were analyzed with the GraphPad software (Version5.01, Graphpad software, San Diego, CA, USA) using log-rank test. Results are represented as the mean ± SD or SEM and $P < 0.05$ was considered statistically significant.

Acknowledgements We thank Professors Hongbing Shu (Wuhan University, Wuhan, China) and Jinxiang Zhang (Wuhan Union Hospital, Wuhan) for providing plasmids and CRC patient samples, respectively. This work was supported by grants from the National Key R&D Program of China (2016YFC1302300) and National Nature Science Foundation of China (81772609, 81802782).

Compliance with ethical standards

Conflict of interest The authors declare that they have no conflict of interest.

References

1. Torre LA, Bray F, Siegel RL, Ferlay J, Lortet-Tieulent J, Jemal A. Global cancer statistics, 2012. CA Cancer J Clin. 2015;65:87–108.
2. Vasaikar S, Huang C, Wang X, Petyuk VA, Savage SR, Wen B, et al. Proteogenomic analysis of human colon cancer reveals new therapeutic opportunities. Cell. 2019;177:1035–49.e19.
3. Cox AD, Fesik SW, Kimmelman AC, Luo J, Der CJ. Drugging the undruggable RAS: mission possible? Nat Rev Drug Discov. 2014;13:828–51.
4. Wee S, Jagani Z, Xiang KX, Loo A, Dorsch M, Yao YM, et al. PI3K pathway activation mediates resistance to MEK inhibitors in KRAS mutant cancers. Cancer Res. 2009;69:4286–93.

5. Ahmed D, Eide PW, Eilertsen IA, Danielsen SA, Eknaes M, Hektoen M, et al. Epigenetic and genetic features of 24 colon cancer cell lines. Oncogenesis. 2013;2:e71.
6. Anastas JN, Moon RT. WNT signalling pathways as therapeutic targets in cancer. Nat Rev Cancer. 2013;13:11–26.
7. Jung YS, Jun S, Kim MJ, Lee SH, Suh HN, Lien EM, et al. TMEM9 promotes intestinal tumorigenesis through vacuolar-ATPase-activated Wnt/beta-catenin signalling. Nat Cell Biol. 2018;20:1421–33.
8. Mercer TR, Dinger ME, Mattick JS. Long non-coding RNAs: insights into functions. Nat Rev Genet. 2009;10:155–9.
9. Batista PJ, Chang HY. Long noncoding RNAs: cellular address codes in development and disease. Cell. 2013;152:1298–307.
10. Gupta RA, Shah N, Wang KC, Kim J, Horlings HM, Wong DJ, et al. Long non-coding RNA HOTAIR reprograms chromatin state to promote cancer metastasis. Nature. 2010;464:1071–6.
11. Taniue K, Kurimoto A, Sugimasa H, Nasu E, Takeda Y, Iwasaki K, et al. Long noncoding RNA UPAT promotes colon tumorigenesis by inhibiting degradation of UHRF1. Proc Natl Acad Sci USA. 2016;113:1273–8.
12. Zhu P, Wu J, Wang Y, Zhu X, Lu T, Liu B, et al. LncGata6 maintains stemness of intestinal stem cells and promotes intestinal tumorigenesis. Nat Cell Biol. 2018;20:1134–44.
13. Sun S, Li W, Ma X, Luan H. Long noncoding RNA LINC00265 promotes glycolysis and lactate production of colorectal cancer through regulating of miR-216b-5p/TRIM44 axis. Digestion. 2019;10:1–10.
14. Ma L, Kuai WX, Sun XZ, Lu XC, Yuan YF. Long noncoding RNA LINC00265 predicts the prognosis of acute myeloid leukemia patients and functions as a promoter by activating PI3K-AKT pathway. Eur Rev Med Pharm Sci. 2018;22:7867–76.
15. Beliakoff J, Sun Z. Zimp7 and Zimp10, two novel PIAS-like proteins, function as androgen receptor coregulators. Nucl Receptor Signal. 2018;4:nrs.04017.
16. Huang CY, Beliakoff J, Li X, Lee J, Li X, Sharma M, et al. hZimp7, a novel PIAS-like protein, enhances androgen receptor-mediated transcription and interacts with SWI/SNF-like BAF complexes. Mol Endocrinol. 2005;19:2915–29.
17. Sharma M, Li X, Wang Y, Zarnegar M, Huang CY, Palvimo JJ, et al. hZimp10 is an androgen receptor co-activator and forms a complex with SUMO-1 at replication foci. Embo J. 2003;22:6101–14.
18. Lee J, Beliakoff J, Sun Z. The novel PIAS-like protein hZimp10 is a transcriptional co-activator of the p53 tumor suppressor. Nucleic Acids Res. 2007;35:4523–34.
19. Rakowski LA, Garagiola DD, Li CM, Decker M, Caruso S, Jones M, et al. Convergence of the ZMIZ1 and NOTCH1 pathways at C-MYC in acute T lymphoblastic leukemias. Cancer Res. 2013;73:930–41.
20. Lee SH, Zhu C, Peng Y, Johnson DT, Lehmann L, Sun Z. Identification of a novel role of ZMIZ2 protein in regulating the activity of the Wnt/beta-catenin signaling pathway. J Biol Chem. 2013;288:35913–24.
21. Possemato R, Marks KM, Shaul YD, Pacold ME, Kim D, Birsoy K, et al. Functional genomics reveal that the serine synthesis pathway is essential in breast cancer. Nature. 2011;476:346–50.
22. Marcotte R, Brown KR, Suarez F, Sayad A, Karamboulas K, Krzyzanowski PM, et al. Essential gene profiles in breast, pancreatic, and ovarian cancer cells. Cancer Discov. 2012;2:172–89.
23. Shen H, Xing C, Cui K, Li Y, Zhang J, Du R, et al. MicroRNA-30a attenuates mutant KRAS-driven colorectal tumorigenesis via direct suppression of ME1. Cell Death Differ. 2017;24:1253–62.
24. Gu L, Zhu Y, Lin X, Li Y, Cui K, Prochownik EV, et al. Amplification of glyceronephosphate *O*-acyltransferase and recruitment of USP30 stabilize DRP1 to promote hepatocarcinogenesis. Cancer Res. 2018;78:5808–19.
25. Cesana M, Cacchiarelli D, Legnini I, Santini T, Sthandier O, Chinappi M, et al. A long noncoding RNA controls muscle differentiation by functioning as a competing endogenous RNA. Cell. 2011;147:358–69.
26. Qu L, Ding J, Chen C, Wu ZJ, Liu B, Gao Y, et al. Exosome-transmitted lncARSR promotes sunitinib resistance in renal cancer by acting as a competing endogenous RNA. Cancer Cell. 2016;29:653–68.
27. Han D, Li J, Wang H, Su X, Hou J, Gu Y, et al. Circular RNA circMTO1 acts as the sponge of microRNA-9 to suppress hepatocellular carcinoma progression. Hepatology. 2017;66:1151–64.
28. Ma P, Yang X, Kong Q, Li C, Yang S, Li Y, et al. The ubiquitin ligase RNF220 enhances canonical Wnt signaling through USP7-mediated deubiquitination of beta-catenin. Mol Cell Biol. 2014;34:4355–66.
29. Novellasdemunt L, Foglizzo V, Cuadrado L, Antas P, Kucharska A, Encheva V, et al. USP7 is a tumor-specific WNT activator for APC-mutated colorectal cancer by mediating beta-catenin deubiquitination. Cell Rep. 2017;21:612–27.
30. Kim J, Alavi Naini F, Sun Y, Ma L. Ubiquitin-specific peptidase 2a (USP2a) deubiquitinates and stabilizes beta-catenin. Am J Cancer Res. 2018;8:1823–36.
31. Yang B, Zhang S, Wang Z, Yang C, Ouyang W, Zhou F, et al. Deubiquitinase USP9X deubiquitinates beta-catenin and promotes high grade glioma cell growth. Oncotarget. 2016;7:79515–25.
32. Wu C, Luo K, Zhao F, Yin P, Song Y, Deng M. et al. USP20 positively regulates tumorigenesis chemoresistance beta-catenin stabilization. Cell Death Differ. 2018;25:1855–69.
33. Shi J, Liu Y, Xu X, Zhang W, Yu T, Jia J, et al. Deubiquitinase USP47/UBP64E regulates beta-catenin ubiquitination and degradation and plays a positive role in Wnt signaling. Mol Cell Biol. 2015;35:3301–11.
34. Li M, Chen D, Shiloh A, Luo J, Nikolaev AY, Qin J, et al. Deubiquitination of p53 by HAUSP is an important pathway for p53 stabilization. Nature. 2002;416:648–53.
35. Luo M, Zhou J, Leu NA, Abreu CM, Wang J, Anguera MC, et al. Polycomb protein SCML2 associates with USP7 and counteracts histone H2A ubiquitination in the XY chromatin during male meiosis. PLoS Genet. 2015;11:e1004954.
36. Wang H, Wang L, Erdjument-Bromage H, Vidal M, Tempst P, Jones RS, et al. Role of histone H2A ubiquitination in Polycomb silencing. Nature. 2004;431:873–8.
37. Saridakis V, Sheng Y, Sarkari F, Holowaty MN, Shire K, Nguyen T, et al. Structure of the p53 binding domain of HAUSP/USP7 bound to Epstein−Barr nuclear antigen 1 implications for EBV-mediated immortalization. Mol Cell. 2005;18:25–36.
38. Yeasmin Khusbu F, Chen FZ, Chen HC. Targeting ubiquitin specific protease 7 in cancer: A deubiquitinase with great prospects. Cell Biochem Funct. 2018;36:244–54.
39. Peuker K, Muff S, Wang J, Kunzel S, Bosse E, Zeissig Y, et al. Epithelial calcineurin controls microbiota-dependent intestinal tumor development. Nat Med. 2016;22:506–15.
40. Morin PJ, Sparks AB, Korinek V, Barker N, Clevers H, Vogelstein B, et al. Activation of beta-catenin-Tcf signaling in colon cancer by mutations in beta-catenin or APC. Science. 1997;275:1787–90.
41. Zhu Y, Gu L, Li Y, Lin X, Shen H, Cui K, et al. miR-148a inhibits colitis and colitis-associated tumorigenesis in mice. Cell Death Differ. 2017;24:2199–209.